30th European Rotorcraft Forum
14-16 September, 2004
Marseilles, France

# SIMULATION OF ROTOR AERODYNAMICS AT HIGH FLIGHT SPEED

**V.A. Anikin, D.S.Kolomenskiy, Yu.N. Sviridenko**
KAMOV Company, Russia

## Abstract

The increase of the incident flow relative velocity results in considerable changes of the rotor airflow behaviour.

The paper discusses traditional assumptions and hypotheses of aerodynamic rotor models and their applicability for high relative velocity regimes. Based on the analysis the paper presents a mathematical model of rotor aerodynamics giving more complete description of its operation. The blade is simulated using a non-linear transient theory of a lifting surface with nonstationary stall zones. A system of skew sections is described to formulate blade spatial flow and to define rotor aerodynamic characteristics. The respective two-dimensional models are used to simulate blade section aerodynamics.

The numerical results are also presented in the paper.

## Introduction

The operation of a rotor at high relative flight speed is characterized by considerable changes in the airflow behaviour.

The problem definition is based on a number of physical conditions that are not taken into account by existing practical theories and models and are usually excluded as hypotheses and assumptions. With speed increase such simplifications of aerodynamic models can lead to considerable errors.

In this connection the paper analyses traditional assumptions and their validity in rotor aerodynamic models for high-speed regimes.

Let's discuss these assumptions and hypotheses.

Spatial airflow. The hypothesis of flat sections normal to the blade axis became an important step in creating practical calculation techniques of rotor aerodynamic characteristics. This hypothesis (S.K. Djevetsky–N.E. Zhukovsky) linked together a rotor blade element and forces acting on it in three-dimensional airflow with an infinite-span (airfoil) wing element in a plane-parallel flow. For fixed-wing aircraft propellers (axial flow) this hypothesis looks natural but for rotors (oblique flow) some constraints (amendments) should be introduced. Practical application of this hypothesis for rotors gives acceptable accuracy up to relative speed of $\overline{V} \sim 0{,}4$. At higher flight speeds radial flows along the blade increase and the spatial airflow should be taken into consideration. Fig. 1 presents the field of velocities near the rotor blades at two flight regimes. The left-side figure shows a flow originated near the rotor at cruise flight regimes. It is seen that the flow slip is not significant enabling to apply traditional hypotheses. At higher flight speed the spatial flow increases, particularly in the area of $\psi = 0 \div 180^{\circ}$ (Fig. 1b).

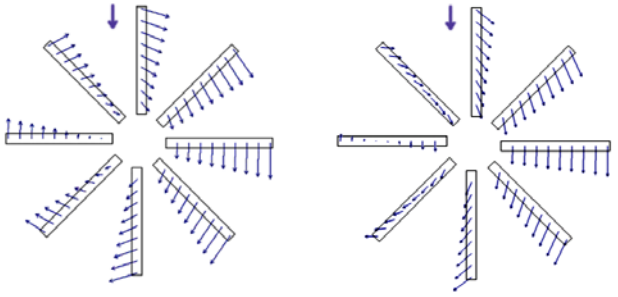

Fig. 1a. Fig. 1b.

To illustrate this phenomenon Table 1 and Fig. 2 give flow slip angles near the rotor at relative radius of 0.5 and 0.9 for various flight speeds. As seen, at low speeds the hypothesis of Djevetsky-Zhukovsky is acceptable but at high speeds the airflow features more spatial nature.

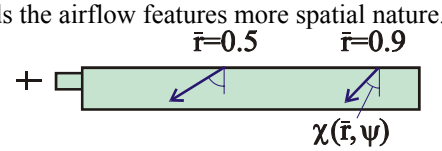


Fig. 2.

Table 1

**χ(r, ψ=0; 180°)**

| V, km/h | $\overline{r}$ =0.5 | $\overline{r}$ =0.9 |
|---|---|---|
| 180 | 27° | 15° |
| 360 | 45° | 29° |
| 450 | 55° | 38° |

«Reverse» flow zone. There are similar reasons to account for reverse flow zone. Up to $\overline{V} \sim 0.4$ the reverse flow zone does not contribute to the calculation of forces and moments; but at higher speed it becomes necessary to involve more complete simulation of blade aerodynamics in the reverse flow zone.

Induction interactions. Vortices interaction with a blade is an important peculiarity of rotor aerodynamics at high speed. As a matter of fact at low and medium flight speed the vortices density is considerable and their interaction is mutually balanced. At higher speed the vortex structure rarefaction increases, it is blown off streamwise, and the intersection of a blade with powerful vortices (fig. 3) causes the stress burst.

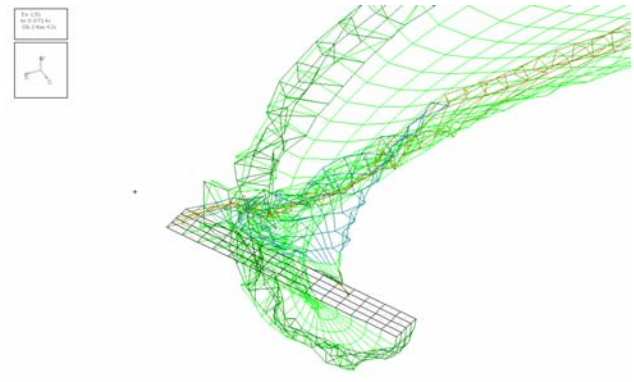

Fig. 3.

More complex interactions are observed for a lower coaxial rotor blade and a vortex sheet off the upper rotor blades. Taking into account that the vortex sheet can approach the blade at various angles, it is necessary to have a more complete model of their interaction.

Blade flow stall. Constant growth of speed and maneuverability characteristics of helicopters is achieved first of all by the rotor capability to produce the g-load of 3÷3,5 and even higher. Such regimes are characterized by large stall flow areas on the blades. The stall flow features transient nature and the stall flow areas vary constantly. These processes are difficult to simulate but this blade flow peculiarity should be accounted for during rotor aerodynamic simulation.

It is necessary to emphasize that stall phenomena reveal themselves mainly at the tip of the retreating blade (hinged rotor) and in the reverse flow area (stall from the sharp blade trailing edge) where the stresses (loads) are not so big. But the vortex sheet coming off the blades in this area results in redistribution of attack angles in other areas and in variation of a blade and rotor aerodynamic performance.

The above discussion of hypotheses shows the necessity of creating a rotor aerodynamic model capable to take account for spatial and transient air flow and blade flow stall at the blade tips and in the reverse flow area.

## Rotor aerodynamics mathematical model

Mathematical model is discussed in detail in (Ref.10). Below is the description of its basic aspects.

Rotor aerodynamic design, i.e. the determination of forces and moments consists of two parts:

1. Determination of circulation along the blade (function of radius and chord) and disturbed velocity field.
2. Determination of rotor aerodynamic forces and moments.

Using a well-known hypothesis of flat sections normal to the blade leading edge, these tasks are split. The solution for the first task is sought for within the theory of ideal fluid, and the influence of viscosity and compressibility is taken into account with $C_x$, $C_y$ airfoil characteristics taken from the experiment (Ref.1).

Let's describe a rotor mathematical model with due account to the discussed above. To take into consideration a spatial flow near a blade let's use the lifting surface theory and a skew section hypothesis will be used for calculating forces and moments. Such approach enables to get an approximation to three-dimensional blade flow and to describe all coefficients of rotor forces and moments with account to spatial flow.

Basic assumptions. At first stage the physical blades are substituted by thin lifting surfaces $S_i$, streamlined with stalled flow from side edges and part of the leading edges (fig 4); special procedures are used to define the flow stall areas.

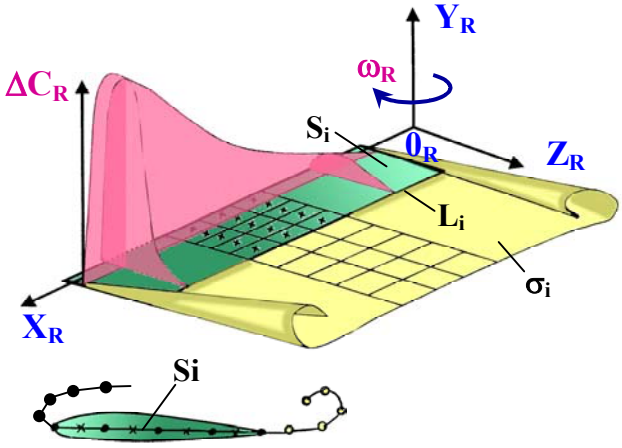


Fig. 4.

Ideal incompressible liquid is considered. No limitations are placed on the blade shape and rotor motion behaviour. The airflow behind the rotor blades generates a developed vortex trail in the form of vortex sheets $\sigma_j$.

A boundary problem is formulated to determine disturbed velocities $\Phi$ (x, y, z, t) satisfying Laplace equation (Ref.2)

$$\frac{\partial^2\Phi}{\partial x^2}+\frac{\partial^2\Phi}{\partial y^2}+\frac{\partial^2\Phi}{\partial z^2}=0,\ (x,y,z)\notin\left(S_i\cup\sigma_j\right)$$

under the following conditions:

- no penetration on basic surfaces;
- pressure continuity and normal velocity component on the surface of a vortex trail;
- Chaplygin-Zhukovsky hypothesis is true for the lifting surface edges $L_j$, from which the vortex sheets $\sigma_j$ flow down;
- at infinite distance from the rotor and its trail the disturbances attenuate.

Vortex sheet deformation to simulate the trail motion in time is described by the ratio

$$(\xi,\eta,\varsigma)=(\xi_1,\eta_1,\varsigma_1)+\int_{\tau_1}^{\tau} w_0(\xi,\eta,\varsigma)\,d\tau,$$

where $(\xi,\eta,\varsigma)$ – are coordinates of sheet points in the point of time $\tau$; $w_0$ – are components of nondimensional media velocity.

To determine the loads on the lifting surfaces a Cauchy-Lagrange integral is used (Ref.3)

$$\frac{\partial\Phi}{\partial t}+\frac{1}{2}(\boldsymbol{W}_0^2-\boldsymbol{W}^{*2})+\frac{p}{\rho}=F(t),$$

where $\boldsymbol{W}_0$, $\boldsymbol{W}^*$ – are vectors of relative and transitional velocities respectively.

Numerical realization of a boundary task is reduced to space and time discretization using discrete vortices method (Ref. 3, 2) by way of replacing continuous discrete

vortex layers with a system of discrete vortices (fig. 5), and time continuous process of changing the boundary conditions and flow parameters is replaced by a stepwise process. The solution of the task in time is based on zero or stationary initial conditions by solving at each time step a system of linear algebraic equations relative to the intensity of attached vortices and calculation of deformation of a trail behind them.

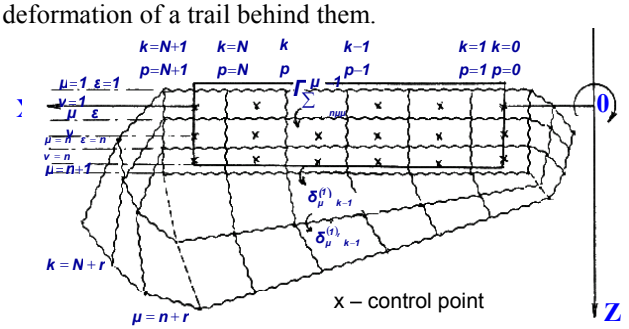


Fig. 5.

The loads determined with Cauchy-Lagrange integral are the first approximation in evaluating the rotor lifting capacity and are the initial data for the second part of the task.

Let's present the numerical results. Fig. 6 shows the diagrams of circulation along the blade length (azimuth ψ=0) at a speed of $\overline{V}$ =0,5 in various rotor blade simulation conditions. The first three calculations do not simulate the reverse flow area, the "lifting surface" differs from the "lifting surface with a side vortex sheet" by the presence of a side sheet at the blade tip. At the same time the side sheet from the blade root was not simulated. The latter version of a "lifting surface with separation in the reverse flow area" the flow is simulated with all side sheets. And in the reverse flow area the sheet comes off from the leading and trailing edges.

To illustrate the interaction of a blade with the tip vortex fig. 7 shows the discreet vortex structure in the discussed regime.

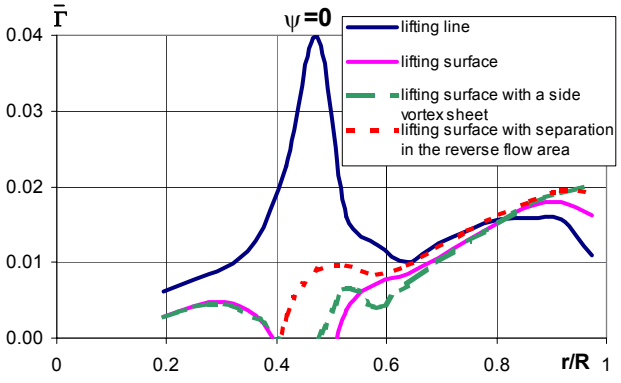


Fig. 6.

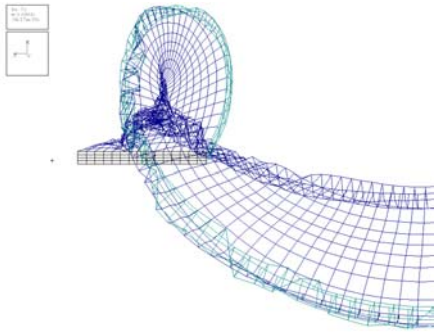

Fig. 7.

Fig. 8 presents the change of the blade thrust in azimuth at large speed $\overline{V}$. The calculation results are presented for three models: in the first one the reverse flow area is not simulated; in the second one the sheet in the reverse flow area comes off from the leading and trailing edges; in the third model the sheet in the reverse flow area comes off from the leading edge only. Flow stall in the reverse flow area has considerable effect on the blade behaviour in this regime.

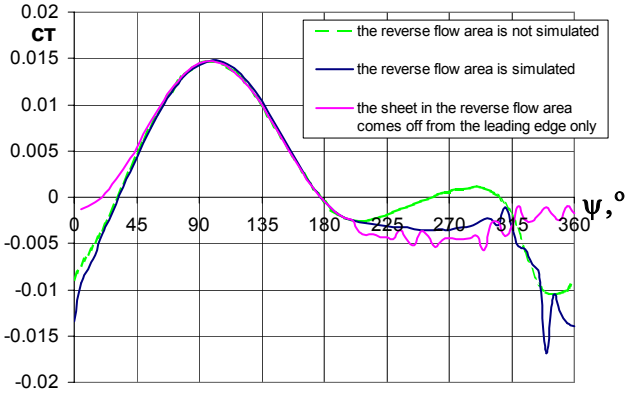


Fig. 8.

Figures 9 and 10 compare the circulation data along the blade length received from the load-bearing line theory at azimuths ψ = 0, 90˚, 180˚, 270˚ and vortex structures for the same regime. As seen from the figures, the relationship between the load distribution behaviour along the blade length and vortex structure in the blade-vortex interaction zone is quite unambiguous.

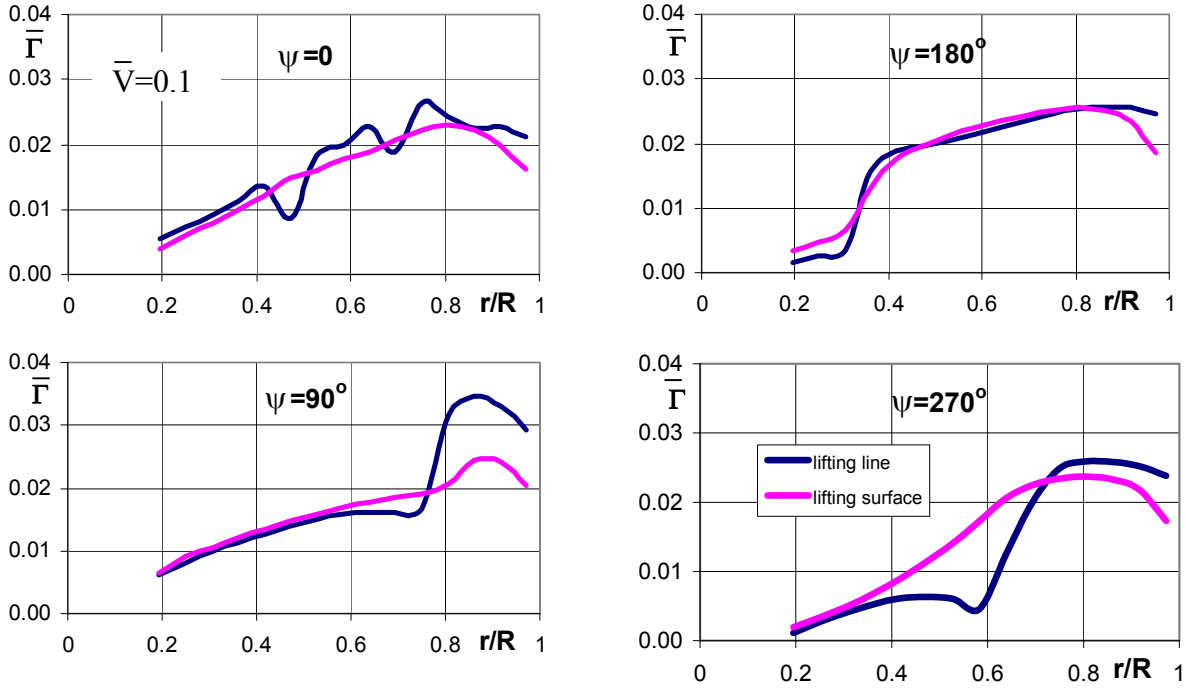


Fig. 9.

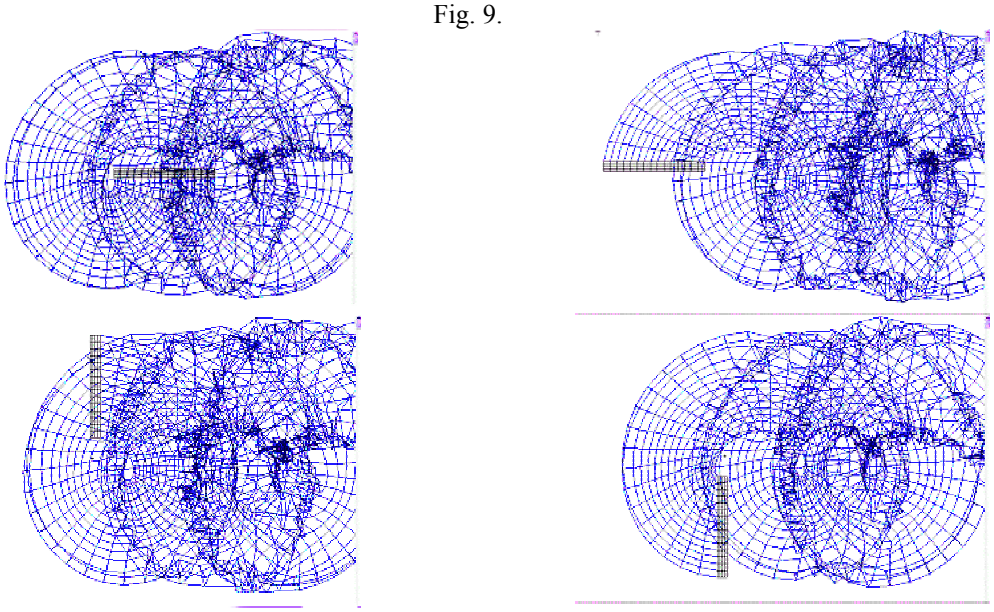

Fig. 10.

The presented materials are sorted out to illustrate the statements formulated at the beginning of the paper and show the influence of the basic factors. As seen, the assumptions used for building a vortex model have essential effect on load distribution and on sheet-blade interaction illustrating the above.

The results of simulation within the used assumptions allow to determine rotor disturbed velocity field that is necessary for completing a procedure of calculating forces and moments.

A method of calculating forces and moments. The velocity fields presented on fig. 1 enable to formulate the main assumption for a model of calculating forces and moments: - the forces acting on lifting surface element in three-dimensional flow are equal to the forces acting on the same element in plane-parallel flow with appropriate flow velocity, slip and attack angles. Formally this is the issue of "flat skew sections" arranged under various slip angles along the rotor blade, fig. 11.

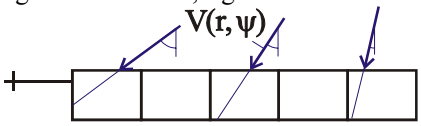


Fig. 11.

By way of building a section along the line of the flow under a certain angle to the blade leading edge we get other airfoils differing from those that make the blade. The situation becomes more complicated when a blade is a twisted blade or it consists of different airfoils. Let's speak about a random airfoil formed by the intersection of physical blade by a flat section at an angle to its leading edge. It remains to formulate a concept of angle of attack of a skew section.

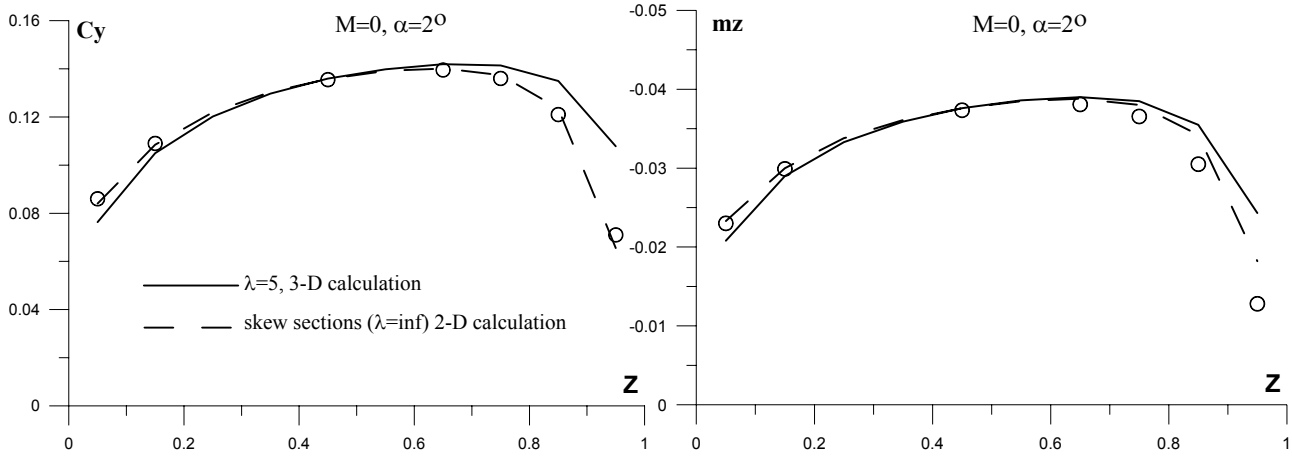


Fig. 12.

Two approaches are feasible: to use the velocity distribution along the airfoil contour or to introduce an averaged angle of attack in the given airfoil. Aiming at model simplification let's introduce an averaged effective angle of attack of a flat section using the transformation of lifting surface into a carrier line. In this case, in accordance with a theory of carrier line, the inductive skew enables to determine the section angle of attack for which the airfoil characteristics are calculated.

This approach takes into account in the first approximation the effect of blade spatial flow on rotor aerodynamic characteristics by way of summing up the elementary forces of flat skew sections.

To justify this procedure the required test numerical investigations were carried out. Using a panel method the flow was calculated for a swept ($\chi$=45°) finite span ($\lambda$=5) wing without taper. Then from all longitudinal vortices the induction skews along 3/4 cord were calculated. The distribution of local angle of attack of the sections taking into account the induction skews from longitudinal vortices was used to calculate the characteristics of infinite moving wing (airfoil) sections.

Fig. 12 shows the distribution of lift coefficient and longitudinal moment of wing sections as compared with the characteristics obtained during three-dimensional wing calculations. Good adjustment of results should be noted. Let's apply another systematical calculation. Heterogeneity of the disturbed velocity field is quite large, and when a vortex approaches a blade it is necessary to specify the changes of boundary conditions along the section length. The results of such adjustments are shown on fig. 12 in the form of circles. It is seen from the figure that in this case the accuracy of the obtained results is practically identical with the case for continuous skew along the section length.

It is worthy to note that the introduction of amendments with account to heterogeneous flow does not cause difficulties in the existing approach.

As a result of refining blade spatial flow a new task is set: to determine airfoil aerodynamic forces. Previously the airfoils that make a blade were tested in wind tunnels and there existed experimental dependencies $C_y$ ($\alpha$, M, Re), $C_{xa}$ ($\alpha$, M, Re) used for calculations, but now we have a huge variety of section profiles and a problem arises to formulate the technique of determining elementary forces of sections of numerous airfoils.

The paper presents a direct technique, i.e. the calculation of aerodynamic performance of an arbitrary airfoil. One of three models is used for this purpose:

- transonic flow around an airfoil;
- unsteady flow around an airfoil;
- steady-state flow around an airfoil.

Let's review these models.

Transonic flow around an airfoil. For approximate description of a transonic flow past an airfoil we shall use a potential flow as a model. As known, the domain of applicability of a potential approximation is limited by Mach number before a sudden change ~1,3÷1,5, and this is acceptable for our model.

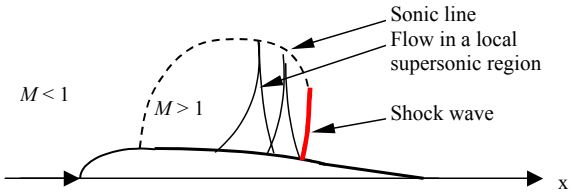


Fig. 13.

To take into account the effect of viscosity on the airfoil surface a system of differential equations that describes gas flow in compressed boundary layer is solved.

A two-layer algebraic turbulence model of Cebeci-Smith is used for determining turbulent transfer coefficients (Ref.6). In accordance with this model the boundary layer is considered to comprise an internal and external areas and their turbulent viscosity coefficients are described by various ratios.

If local stall zones appear on the airfoil surface a special technique is used for transforming boundary layer equations.

The scheme described above was used to calculate aerodynamic characteristics of helicopter blade airfoils.

Fig. 14 illustrates a comparison of drag coefficient of a helicopter airfoil within a wide range of Mach numbers.

Fig. 15 compares pressure distribution for another helicopter airfoil obtained in calculation and in experimental test in T – 106M wind tunnel of TsAGI.

On the whole a good convergence should be marked, however in some calculations (at large Mach numbers, α) there is a bad convergence of a solution with account for viscosity.

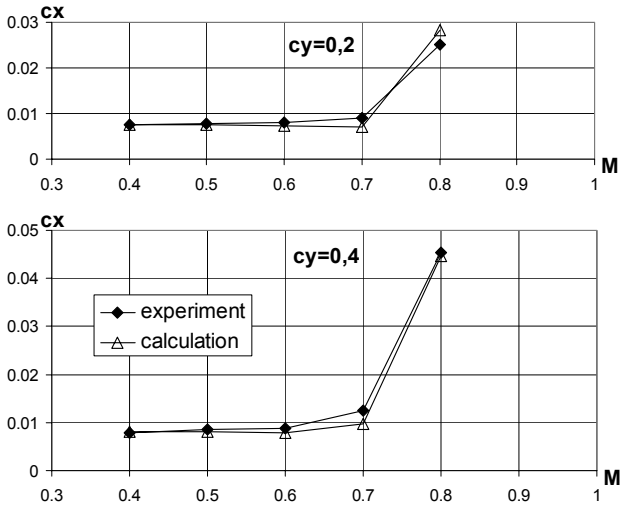


Fig. 14.

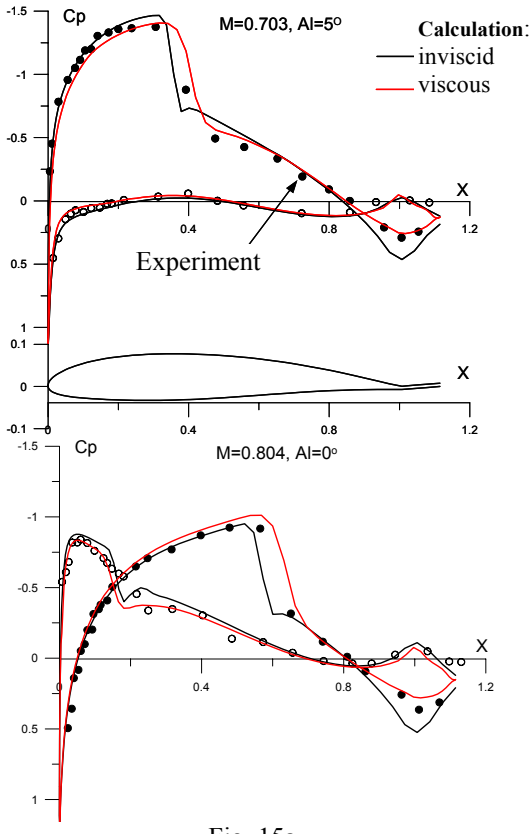


Fig. 15a.

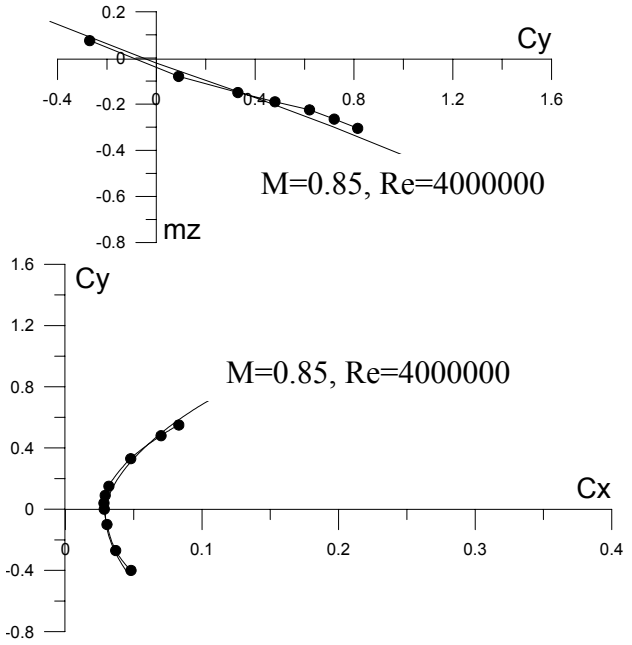


Fig. 15b.

Unsteady airflow around an airfoil. Essentially almost all rotor operation regimes can be referred to as unsteady regimes. This is the determining characteristic of rotor operation. Only a small airflow area of the advancing blade can be considered as quasi-steady. Let's use calculation method for a stalled airflow as a model (Ref.2,3,7,10). The flow is divided into two areas (models) of non-viscous noncompressible flow and non-steady boundary layer.

A method of discreet vortices is used to calculate flow parameters in the area of non-viscous flow. Discreet vortices are located on the airfoil surface, between the vortices there are test points in which the boundary no penetration and Thompson circulation consistency conditions are met and a regularizing variable (Ref.3) is introduced to eliminate the overdetermination of equation system.

The flow parameters in the area of viscous flow are determined by way of numerical integration of a system of differential equations of non-steady boundary layer (Ref.2,3,4).

The boundary layer is calculated from the critical point (fig. 16) to the stall point (R). As described in (Ref.3), the regimes with several critical points are feasible.

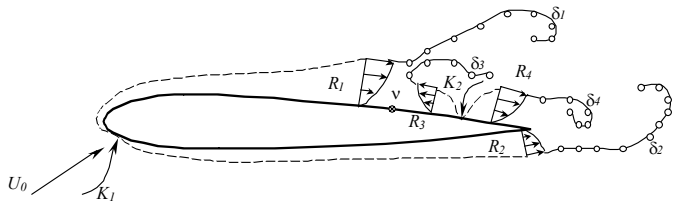


Fig. 16.

The aerodynamic loads on the section profile are calculated at each time step using Cauchy-Lagrange integral.

The profile contour integrals of pressure coefficients and skin friction allow to calculate aerodynamic force coefficients $C_y$, $C_x$ and longitudinal moment relative to the leading edge.

Let's examine the results of computational investigation of airfoil non-steady characteristics and their comparison with experimental data.

Fig. 17 shows the dependencies of airfoil lift coefficients versus angle of attack $C_y(\alpha)$ for NACA-0012 airfoil when the angle of attack changes according to the law $\alpha=15+10\sin 0{,}3\tau$, for Re=4000000. The same figure presents the experimental data (Ref.5). When the angle increases the normal force coefficient of the airfoil increases in accordance with the law similar to a linear law and considerably exceeds maximum values of steady-state airflow. When moving in reverse direction the nonlinearity and noticeable load fluctuations appear. On the whole the computation describes satisfactorily the experimental dependence. Figures 18 and 19 show design and experimental (Ref.9) non-steady characteristics $C_y$, $m_z$ of V-230-10 airfoil.

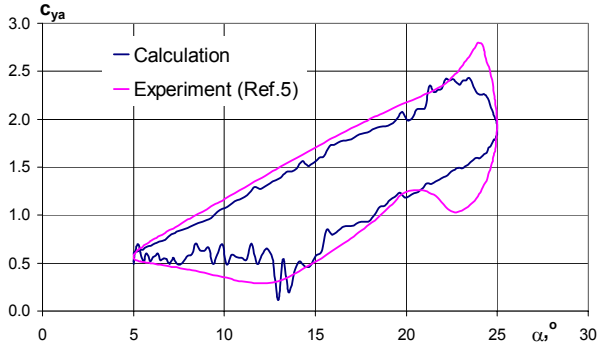


Fig. 17.

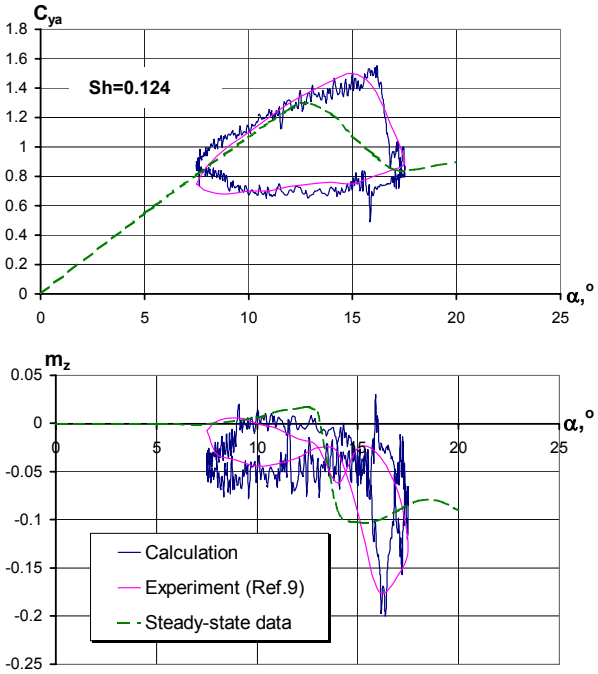


Fig. 18.

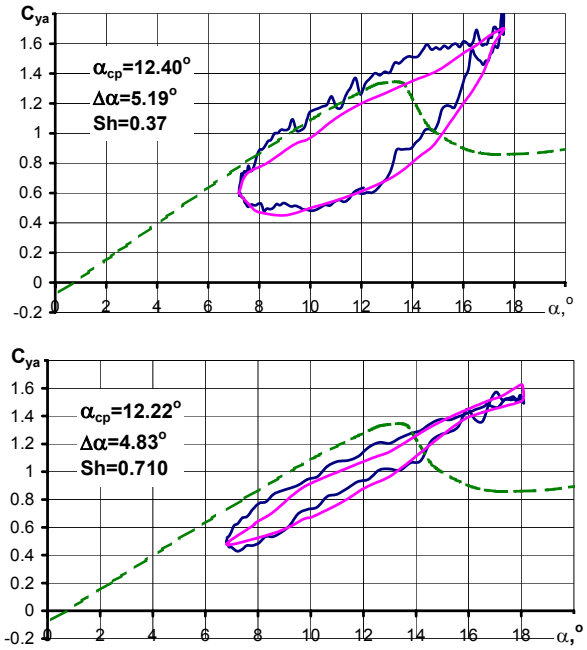


Fig. 19.

For all cases the aerodynamic load fluctuations are registered that implies the introduction of regularizing numerical procedures.

With higher Mach number the non-steady state effect decreases and for transonic flow around the airfoil a steady-state model is substantiated.

Steady-state airflow around an airfoil. Steady-state airflow will be a specific solution of the above methods. However the application of these airfoil aerodynamic models at all regimes will require higher computational power. New approaches are being developed to reduce the labour intensiveness of computations (Ref.8).

Aerodynamic coefficients. The forces and moments on the rotor are determined in accordance with traditional scheme of summing up elementary forces and moments of the rotor sections (Ref.1). The difference is the account for flow slip along the rotor length; as a result the computation is based on skew sections. For quasi-static flows the elementary forces in skew section are computed with specified $\alpha$, M and Re values. For non-stationary flow around the airfoil the flow "history" is used. That means that functions $\alpha$ (r), V (r) are introduced that remember the change of kinematic parameters during a certain previous period of time. "Real" $\alpha$ functions, V = f(t), or their Fourier series expansions can be used for computing non-stationary characteristics.

As an illustration fig. 20 presents the comparison of calculated rotor aerodynamic characteristics with the experimental data obtained in a wind tunnel for a large scale model at full scale Mach numbers. In the simulation it was assumed that no airflow separation from the blades occurred.

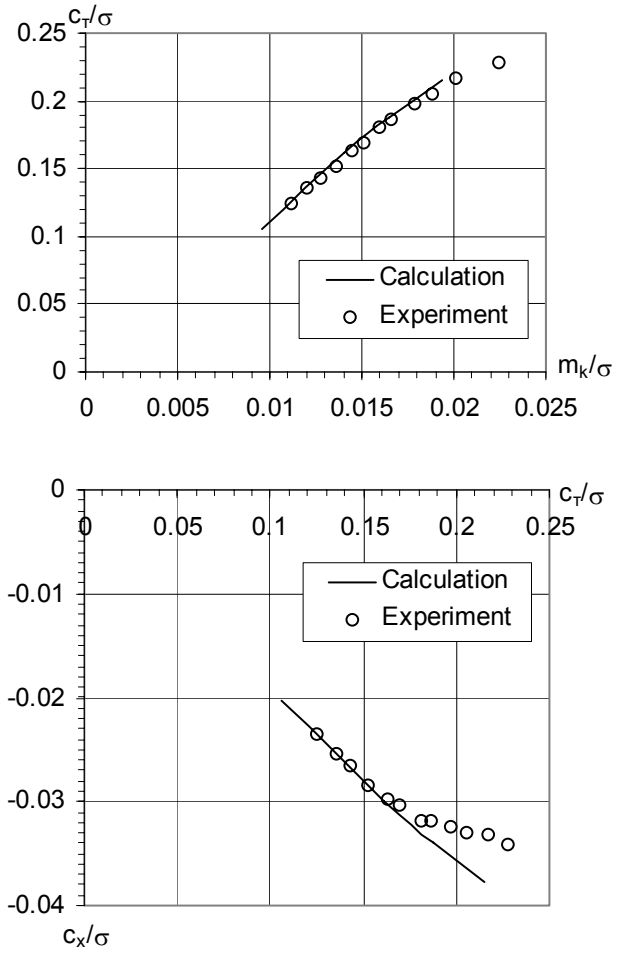


Fig. 20.

## Conclusions

In conclusion let's formulate the basic results.

1. A rotor(s) mathematical model is proposed that takes into account a number of important physical factors and expands the aerodynamics simulation domain.

First of all it allows for more comprehensive simulation of rotor aerodynamics at high speed and g-loads.

2. Traditional hypothesis such as flat sections, normal to the blade leading edge and experimental wind tunnel tests of the airfoils making the blade are not used within the proposed model.
3. A method of taking into account spatial flow around rotor blade and its effect on rotor aerodynamics is proposed.
4. Within the lifting surface theory used for simulating rotor blade aerodynamics a way of calculating all force and moment components is proposed.
5. Verification data of the main components of a mathematical model and results of relevant experiments are presented enabling to forecast the availability of the described mathematical model for practical tasks.

## References

[1] Theory of a Rotor, Moscow: Mashinostroenie, 1973.

[2] Kritsky B. Anikin V., Multilevel Mathematical Model of Rotorcraft Aerodynamics. 27th European Rotorcraft Forum, Moscow, 2001.

[3] Belotserkovsky S., Kotovsky V., Nisht M., Fedorov R. Mathematical Modelling of Stalled Flow Around a Body. M.: Science, 1988.

[4] Schlichting G. Boundary Layer Theory M.: Sience, 1974.

[5] Carr L.M. Progress in Analysis and Prediction of Dynamic Stall. J. of Aircaft # 1, 1988.

[6] Cebeci T., Bradshaw P. Convective Heat Transfer. M.: «World», 1987.

[7] Gerasimov O., Kritsky B. Simulation of Stall Flow Around Helicopter Rotor Blade. Proceedings of the 3rd Forum of the Russian Helicopter Society and Juriev Lectures. M.: Russian helicopter Society, 1980.

[8] Anikin V., Sviridenko Yu. Application of Artificial Neural Networks for Designing and Determination of Aerodynamic Characteristics of Helicopter Rotor Airfoils. Proceedings of the 6th Forum of the Russian Helicopter Society. M., 2004.

[9] Liiva J., Davenport F.J., Gray L., Walton I.C. Two-Dimensional Tests of Airfoils Oscillating Near Stall. Volume 1. Summary and evaluation of results. USAAVLABS TR 68-13A. Philadelphia, Pennsylvania, 1968.

[10] Anikin V., Gerasimov O., Kolomenskiy D., Kritsky B., Sviridenko J. A Method of Aerodynamic Design of a Rotor. Proceedings of the 6th Forum of the Russian Helicopter Society. M., 2004.